Climatological SST and MLD Predictions from a Global Layered Ocean Model with an Embedded Mixed Layer*

A. BIROL KARA, ALAN J. WALLCRAFT, AND HARLEY E. HURLBURT

Naval Research Laboratory, Stennis Space Center, Mississippi

(Manuscript received 18 October 2001, in final form 16 April 2003)

ABSTRACT

The Naval Research Laboratory (NRL) Layered Ocean Model (NLOM) with an embedded mixed layer submodel is used to predict the climatological monthly mean sea surface temperature (SST) and surface ocean mixed layer depth (MLD) over the global ocean. The thermodynamic model simulations presented in this paper are performed using six dynamical layers plus the embedded mixed layer at 1/2° resolution in latitude and 0.703125° in longitude, globally spanning from 72°S to 65°N. These model simulations use climatological wind and thermal forcing and include no assimilation of SST or MLD data. To measure the effectiveness of the NLOM mixed layer, the annual mean and seasonal cycle of SST and MLD obtained from the model simulations are compared to those from different climatological datasets at each grid point over the global ocean. Analysis of the global error maps shows that the embedded mixed layer in NLOM gives accurate SST with atmospheric forcing even with no SST relaxation/assimilation. In this case the model gives a global root-mean-square (rms) difference of 0.37°C for the annual mean and 0.59°C over the seasonal cycle over the global ocean. The mean global correlation coefficient (R) is 0.91 for the seasonal cycle of the SST. NLOM predicts SST with an annual mean error of <0.5°C in most of the North Atlantic and North Pacific Oceans. For the MLD the model gave a global rms difference of 34 m for the annual mean and 63 m over the seasonal cycle over the global ocean in comparison to the NRL MLD climatology (NMLD). The mean global R value is 0.62 for the seasonal cycle of the MLD. Additional model–data comparisons use climatological monthly mean SST time series from 18 National Oceanic Data Center (NODC) buoys and 11 ocean weather station (OWS) hydrographic locations in the North Pacific Ocean. The median rms difference between the NLOM SSTs and SSTs at these 29 locations is 0.49°C for the seasonal cycle. Deepening and shallowing of the MLD at the all OWS locations in the northeast Pacific are captured by the model with an rms difference of <20 m and an R value of >0.85 for the seasonal cycle.

Using several statistical measures and climatologies of SST and MLD we have demonstrated that NLOM with an embedded mixed layer is able to simulate with substantial skill the climatological SST and MLD when using accurate and computationally efficient surface heat flux and solar radiation attenuation parameterizations over the global ocean. Further, this was accomplished using a model with only seven layers in the vertical, including the embedded mixed layer. Success of climatological predictions from the NLOM with an embedded mixed layer is a prerequisite for simulations using interannual atmospheric forcing with high temporal resolution. NLOM gives accurate upper-ocean quantities with atmospheric forcing even with no SST relaxation or assimilation, a strong indication that the model is a good candidate for assimilation of SST data. Finally, the techniques and datasets used here can be applied to evaluation of other ocean models in predicting the SST and MLD.

1. Introduction and motivation

Many ocean modeling studies of the past have helped lay the foundation for understanding the ocean's role in climate change in many different aspects. Among these aspects an adequate understanding of climatological sea surface temperature (SST) and ocean mixed layer depth (MLD) variability and the ability to simulate and predict them are important (e.g., Cherniawsky and Holloway 1991; Schopf and Loughe 1995). In order to predict SST and MLD it is necessary to analyze the effects of surface heat flux and surface ocean mixed layer physics, but observations are not adequate to carry out such extensive diagnostic studies at present. In these cases, simulations from ocean general circulation models (OGCMs) that can accurately simulate SST and MLD may be useful in compensating for the sparseness of the oceanic observations and provide a more comprehensive picture.

Most bulk mixed layer models are one-dimensional and assume that the mean temperature and horizontal velocity are quasi-uniform within the layer, but have a jump at the lower boundary (e.g., Niiler and Kraus 1977; Price et al. 1986; Garwood 1977). To close the model the entrainment velocity at the base of the mixed layer

* Naval Research Laboratory Contribution Number JA/7320/01/0025.

Corresponding author address: A. Birol Kara, Naval Research Laboratory, Code 7323, Stennis Space Center, MS 39529-5004.
E-mail: kara@nrlssc.navy.mil

© 2003 American Meteorological Society

is prescribed in terms of the wind stress and/or the velocity and density difference between the mixed layer and water below it. This type of prescription is chosen because a surface mixed layer develops that has approximately uniform density, when the wind blows across a stratified ocean (Kara et al. 2000a) and the density jump across the bottom of the mixed layer increases as the mixed layer depth increases (Li and Garrett 1997). The main disadvantage of these models is that the surface mixed layer suffers from inadequate physics for the mixed layer deepening and thereby SST prediction. The NLOM with an embedded mixed layer has several advantages in this regard. For example, although the mixed layer formulation is based on the bulk mixed layer approach, and thus originates from the Kraus and Turner (1967) formulation, it has a convection option not found in traditional bulk models, which allows an unstable mixed layer to deepen. In addition, the stable depth in the model is based on the temperature profile extending through the dynamic layers. If there is surface heating, no special action is taken since heating and mixing already have a tendency to warm and shallow the mixed layer.

In this paper we demonstrate the capability of the NLOM mixed layer model to predict climatological mean SST and MLD. A reasonable criterion for the reliability of a global OGCM's mixed layer is its ability to simulate upper-ocean characteristics over the global ocean. A heat flux difference of 25 W m^{-2} can change the temperature of 50 m of water by over 3.5° yr^{-1} (Blanc 1987). Such a large error would be intolerable in an OGCM integration. Thus, uncertainities in the heat flux data would dominate the model results to a large extent. This implies that reliable predictions of SST and MLD require accurate flux forcing as well. In addition, from the global ocean modeling point of view, model parameters need to be optimal and to work well globally in predicting upper-ocean quantities.

A set of evaluation criteria is needed for a convincing assessment of an OGCM mixed layer. Most one-dimensional mixed layer modelers have limited their model–data comparisons to their area of interest, and they have typically used observations at only a few locations for the model verification (e.g., Martin 1985; Kantha and Clayson 1994). However, it is obvious that verifying results from a global ocean model at a single location is not very informative in measuring a model's skill and cannot provide adequate evaluation of the model success or its deficiencies (e.g., Murtugudde et al. 1995; Hu and Chao 1999). In this paper, we set up a standard for those model–data comparisons by presenting various statistical measures that are applied to each ocean grid over the global ocean. Further, we analyze zonally averaged measures to obtain a general picture of model deficiencies as a function of latitude.

Organization of this paper is as follows. Section 2 briefly introduces the mixed layer model parameterizations along with the climatological forcing fields used and simulations performed. Section 3 presents comparisons of SST and MLD obtained from the NLOM with climatological SST and MLD fields. Section 4 further illustrates model–data comparisons at many individual buoy and ocean weather stations located at different places in the global ocean. The conclusions of this study are in section 5.

2. Mixed layer model

The thermodynamic version of the NLOM uses a primitive equation layered formulation where the equations have been vertically integrated through each Lagrangian layer. Prognostic variables are layer density, layer thickness, and layer volume transport per unit width (layer velocity times layer thickness). The model has six dynamical layers plus the mixed layer and realistic bottom topography is confined to the lowest layer in the simulations reported here. A bulk-type mixed layer submodel is embedded within the NLOM. It is an independent submodel loosely coupled to NLOM's dynamical core, requiring only near-surface currents, the temperature just below the mixed layer, and an estimate of the stable mixed layer depth. The model domain used for this study includes the global ocean at all longitudes from 72°S to 65°N, gridded to a resolution of 0.5° in latitude and 0.703125° in longitude and has lateral boundaries that follow the 200-m isobath with a few exceptions.

In this paper, we give only a brief description of the embedded mixed layer parameterizations. The reader is referred to Wallcraft et al. (2003, this issue) for a full description of the model formulations, Kara et al. (2000b) for computational efficiency of thermal flux parameterizations, and Kara et al. (2002a) for the parameterizations used for calculating atmospheric forcing fields. The embedded mixed layer model employed here carries prognostic equations for the SST (T_m) and MLD (h_m) as follows:

$$\frac{\partial T_m}{\partial t} + \mathbf{v}_1 \cdot \boldsymbol{\nabla} T_m = -\frac{\max(0, \omega_m)}{h_m}(T_m - \Delta T_m - T_b) + \frac{Q_a - Q_P e^{-h_m/h_P}}{\rho_0 C_{\mathrm{pa}} h_m} + \frac{K_H}{h_m}\boldsymbol{\nabla} \cdot (h_m \boldsymbol{\nabla} T_m) \quad \text{and} \tag{1}$$

$$\frac{\partial (h_m)}{\partial t} + \boldsymbol{\nabla} \cdot (h_m \mathbf{v}_1) = \omega_m. \tag{2}$$

A brief description of variables appearing in Eqs. (1) and (2) are provided in Table 1. Major free parameters in these equations are net surface heat flux (Q_a), temperature difference at the base of the mixed layer [$\Delta T_b = (T_m - \Delta T_m) - T_b$], and vertical mixing velocity (ω_m). These free parameters are obtained from the surface energy budget, a continuous model temperature profile,

TABLE 1. Model variables and constants along with their units in the Système Internationale (SI).

Symbol	Description of variable used in model formulation
C_{pa}	Specific heat of air (1004.5 J kg^{-1} K^{-1})
h_m	Mixed layer depth (m)
h_P	Radiation absorption length scale (m)
K_H	Coefficient of horizontal temperature diffusivity (0 m^2 s^{-1})
Q_a	Net heat flux at the ocean surface (W m^{-2})
Q_P	Penetrating solar radiation (W m^{-2})
t	Time (s)
T_b	Temperature just below the mixed layer (°C)
T_m	Sea surface temperature (°C)
$\mathbf{v}_1$	Layer 1 velocity (m s^{-1})
ΔT_m	Temperature change across the mixed layer (°C)
ω_m	Vertical mixing velocity (m s^{-1})
ρ_0	Reference density (1000 kg m^{-3})
Symbol	**Mixed layer model constant**
C_{pw}	Specific heat of water (3993 J kg^{-1} K^{-1})
f^+	Coriolis parameter at 5° lat (2.5 × 10^{-5} s^{-1})
h_m^+	Minimum mixed layer depth (10 m)
L_v	Latent heat of vaporization (2.5 × 10^6 J kg^{-1})
m_i	TKE constants (m_1 = 6.25, m_3 = 7.5, m_5 = 6.3, m_6 = 0.3)
n_c	TKE constant (n_c = 1)
P_a	Atmospheric pressure at sea surface (1013 mb)
R_{gas}	Gas constant (287.1 J kg^{-1} K^{-1})
$\mathbf{v}_a^+$	Minimum wind speed (4 m s^{-1})
ΔT_b^+	Minimum temperature difference at the base of the mixed layer (0.2°C)

and a modified Kraus–Turner model, respectively (Wallcraft et al. 2003).

A minimum value (10 m) is imposed on the MLD [Eq. (2)] because the formulation is not accurate for very shallow mixed layers. The temperature change across the mixed layer is ΔT_m, which is specified as a function of latitude based on the Naval Research Laboratory mixed layer depth (NMLD) climatology (Kara et al. 2003), which was constructed based on an optimal layer depth definition (Kara et al. 2000a). The values range from 0.1°C at high latitudes to 1.5°C at low latitudes (Kara et al. 2002b).

The thermal forcing formulation used here for latent and sensible heat fluxes at the air–sea interface is similar to that used by Kara et al. (2002a), which was validated against the Tropical Ocean Global Atmosphere Coupled Ocean–Atmosphere Response Experiment (TOGA COARE) algorithm (Fairall et al. 1996), which is much more computationally expensive. The surface solar irradiance is decomposed into its infrared (Q_{IR}) and penetrating radition, so-called photosynthetically available radiation (PAR). Thus, the net surface heat flux forcing includes the attenuation of the shortwave radiation with depth (Rochford et al. 2001).

The annual climatological SST cycle is built into the model to a limited extent. Including air temperature in the formulations for the latent and sensible heat flux (Kara et al. 2002a) model SST automatically provides a physically realistic tendency toward the ''correct'' SST. There is no explicit SST relaxation term in the prognostic SST equation, but entrainment at the base of the mixed layer allows the dynamical layer density relaxation to influence SST. Below the mixed layer, the density of the top dynamical layers is relaxed toward the annual mean climatological density of that layer except for layer 1. The latter is relaxed toward a monthly mean climatology interpolated to daily values due to the significant seasonal cycle within that layer. This is feasible in NLOM because most of the information about circulation anomalies is carried by layer thickness anomalies, not density anomalies. Jacobs et al. (1994) showed NLOM with density relaxation maintaining an El Niño–generated Rossby wave for over a decade. The problem with doing this in layer 1 without heat fluxes (and in all deeper layers) is that there is a phase lag between applying the relaxation and it having an effect. However this problem usually goes away with heat fluxes since in principle the difference between the model layer 1 temperature and the climatological layer 1 temperature is then small (e.g., due to interannual variation). In fact, relaxing to an annual climatology, while certainly maintaining the long-term mean, tends to act against the heat-flux-generated layer 1 seasonal cycle. As a consequence, the net surface heat fluxes usually follow a repeatable annual cycle that deviates only when there are large changes in the model SST and MLD, a situation also reported in other studies (e.g., Seager et al. 1988).

All model simulations are performed with climatological 6-hourly hybrid winds that consist of monthly Hellerman and Rosenstein (1983) wind stresses (HR) and European Centre for Medium-Range Weather Forecasts (ECMWF) wind anomalies (Wallcraft et al. 2003). In addition to the wind forcing, the model also uses climatological thermal forcing. In this case, climatological monthly means of the shortwave plus longwave radiation, air temperature (T_a), and air mixing ratio (q_a) are obtained from the Comprehensive Ocean Atmosphere Data Set (COADS) as described in da Silva et al. (1994).

Model simulations presented in this paper are performed with no assimilation of SST and MLD data. The six-layered thermodynamic model without the mixed layer is spun up to statistical equilibrium. The model run is then extended for 5 yr with the mixed layer. Since this run reaches statistical equilibrium in just a few years, it was possible to perform many sensitivity studies and to tune mixed layer model parameters. An optimal set of model parameters used in the simulations is provided by Wallcraft et al. (2003) along with reasons for these choices. The resulting mixed layer model constants are given in Table 1.

3. Model–data comparisons

For evaluation of the model results, monthly means of SST and MLD are formed from January through

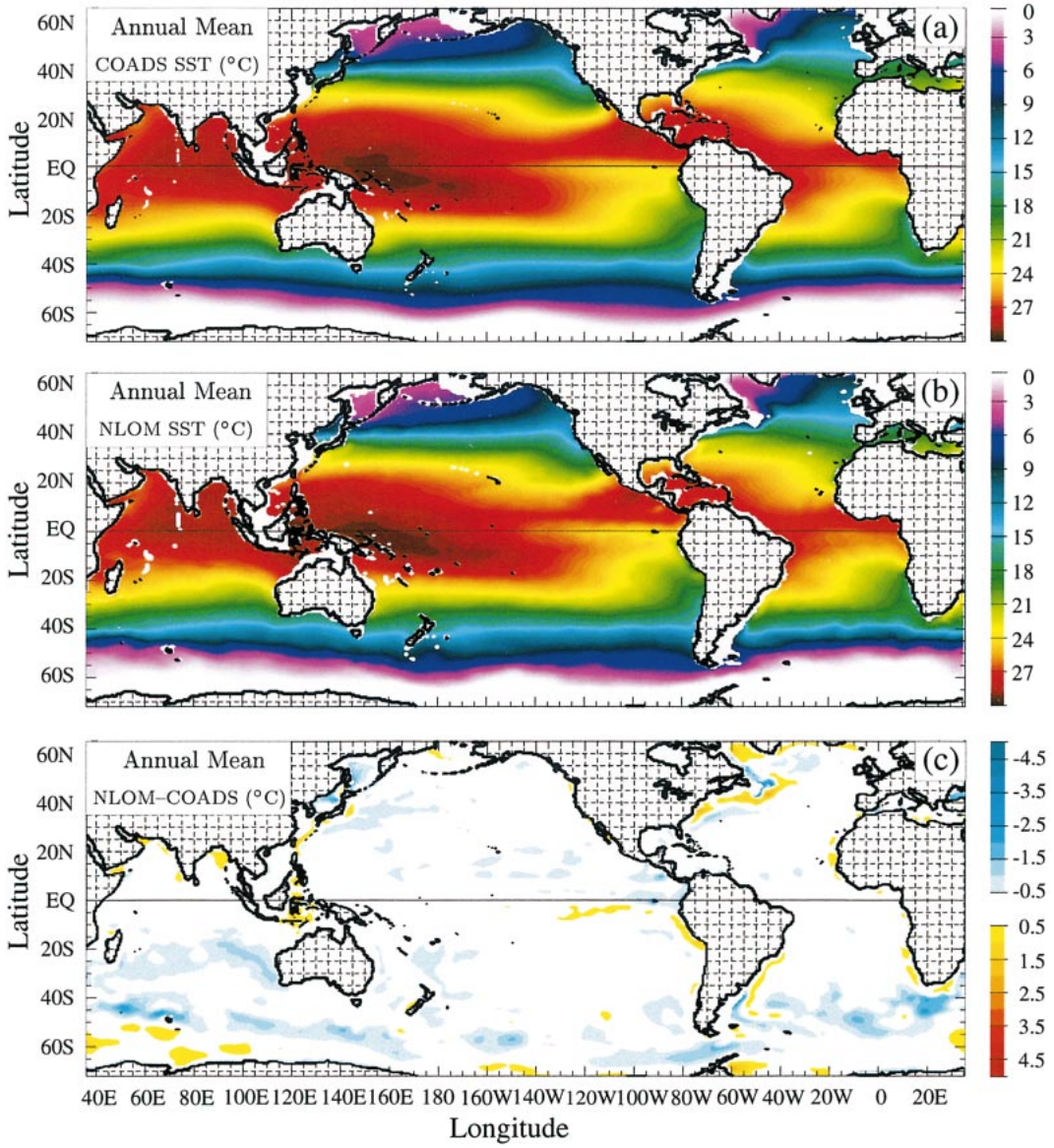

FIG. 1. Comparison of annual mean SST at each model grid point over the global ocean. (a) Annual mean climatological SST from COADS, (b) annual mean simulated SST from NLOM, and (c) annual mean error (ME) between the NLOM and COADS SST. Note that SST in the Antarctic is less than 0°C, and it is shown as white. Global average of annual SST mean error is −0.15°C, and the global rms difference is 0.37°C.

December using the fifth model year. These values are then compared to climatology at each grid point of the global ocean. It was possible to use only one year for this purpose because the ½° model is largely deterministic and flow instabilities make only a minor contribution at this resolution.

Several statistical measures are considered together to assess the comparison between SST values predicted by the model (NLOM SST) and those from the climatology (COADS SST). A similar comparison is made later for MLD. Let $X_i (i = 1, 2, \ldots, n)$ be the set of n reference values (i.e., COADS SST), and let $Y_i (i = 1, 2, \ldots, n)$ be the set of estimates (i.e., NLOM SST). Also let $\overline{X}(\overline{Y})$ and $\sigma_X(\sigma_Y)$ be the mean and standard deviations of the reference (estimate) values, respectively. For model–data comparisons we evaluate time series of monthly mean SST values from January to December at each grid point over the global ocean; thus, n is 12. Given these definitions, following Stewart (1990) and Murphy (1988) the statistical relationships between COADS SST (X) and NLOM SST (Y) can be expressed as follows:

$$\mathrm{ME} = \overline{Y} - \overline{X}, \tag{3}$$

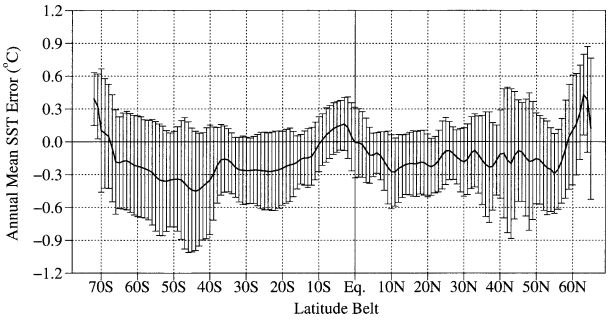

FIG. 2. The zonally averaged annual mean differences between NLOM and COADS SST values (see Fig. 1c). The annual mean is calculated using 12 monthly averages from January to December at each model grid point, and the zonal averaging is performed at each 1° latitude belt from 72°S to 65°N over the global ocean. Also included are the ± std devs of the zonally averaged annual mean differences for each latitude belt.

$$\mathrm{RMS} = \left[\frac{1}{n}\sum_{i=1}^{n}(Y_i - X_i)^2\right]^{1/2}, \tag{4}$$

$$R = \frac{1}{n}\sum_{i=1}^{n}\frac{(X_i - \overline{X})(Y_i - \overline{Y})}{(\sigma_X\sigma_Y)}, \quad \text{and} \tag{5}$$

$$\mathrm{SS} = R^2 - \underbrace{[R - (\sigma_Y/\sigma_Z)]^2}_{B_C} - \underbrace{[(\overline{Y} - \overline{X})/\sigma_X]^2}_{B_{\mathrm{UC}}}, \tag{6}$$

where ME is the bias or annual mean difference, RMS is the root-mean-square difference, R is the correlation coefficient, and SS is the skill score. For 12-monthly SST at each grid point over the global ocean the R value between NLOM and COADS SST must be at least ± 0.53 for it to be statistically different from an R value of zero based on a Student's t test at a 95% confidence interval (Neter et al. 1988). We note here that the null hypothesis significance testing tells us little of what we really need to know and might be inherently misleading (Nicholls 2001). However, it is still helpful for our purposes when evaluating the significance of correlations over the global ocean because one possible use of this hypothesis occurs where correlations are displayed in a map, as is done in this paper.

The SS in Eq. (6) is computed by accounting for two biases, termed conditional and unconditional bias. Unconditional bias (also called systematic bias) is a measure of the difference between the means of NLOM SST and COADS SST, while conditional bias is a measure of the relative amplitude of the variability in the two datasets (Murphy 1992). The SS based on rms difference can be defined as $\mathrm{SS} = 1 - \mathrm{RMS}^2/\sigma_X^2$ and this is mathematically equivalent to Eq. (6). The SS is 1.0 for perfect NLOM SSTs (e.g., Murphy and Daan 1985) and positive skill is usually considered to represent a minimal level of acceptable performance. Note that the correlation coefficient squared is equal to SS only when the conditional and unconditional biases are zero. Because the two biases are never negative, the correlation can be considered to be a measure of ''potential'' skill, that is the skill that can be obtained by eliminating bias from the NLOM.

Using the preceding statistical measures we will perform model–data comparisons for SST and MLD, separately. We note here that the current version of the NLOM mixed layer does not simulate the diurnal cycle so there is no need to form a daily average of model SST and MLD and then form monthly means. Therefore, monthly mean model SST and MLD are obtained by averaging the values at each model output interval (3.05 days) for each month (i.e., 10 outputs per month).

a. Sea surface temperature

The ability of NLOM to reproduce the climatological SST is first evaluated in terms of the annual mean using the climatological COADS SST (Fig. 1a) and the corresponding NLOM SST (Fig. 1b). The departure of model SST from the climatological SST (Fig. 1c) illustrates that ME is less than ± 0.5°C over most of the global ocean. In fact, the global average of the ME and the global rms difference between the annual mean NLOM and COADS SSTs are only -0.15° and 0.37°C, respectively.

The SST errors in the open ocean are usually smaller than those along continental boundaries and the equatorial upwelling region between 80° and 100°W. However, SST features along continental boundaries are not well resolved by either the 1/2° model or the climatology, and the errors are still on the order of 1°C in these regions. The large latitudinal divergence in the equatorial surface currents forces upwelling into the mixed layer, which in turn results in shallowing of MLD (see section 3b). Figures 1a and 1b also show that the southeastern region in the equatorial ocean is characterized by water getting colder eastward toward the coast and southward to higher latitudes.

The annual mean model SST is cool by about 0.5°–1°C in the North Pacific Ocean, where the Kuroshio Current system is located, and 0.5°–2°C in the North Atlantic Ocean where the Gulf Stream is located and in some regions of the Southern Ocean. The weak Gulf Stream and its overshoot of the separation latitude in the northwestern Atlantic Ocean simulated by the ½° NLOM leads to SSTs that are ≈1°C colder or warmer than the climatology, similarly for the Kuroshio. Although a few other current systems, such as Oyashio and Labrador, are not resolved well in the ½° version of the NLOM in comparison to a higher resolution of NLOM (Hurlburt et al. 1996; Metzger and Hurlburt 1996), we do not see large errors associated with these current systems. The mean SST errors in the warm pool and Antarctic are small. Knowing that NLOM has not been coupled with an ice model as in, for example, Yuen et al. (1992), and that there is no special treatment for the existence of ice in the model-calculated sensible and latent heat fluxes, the model's SST errors of less

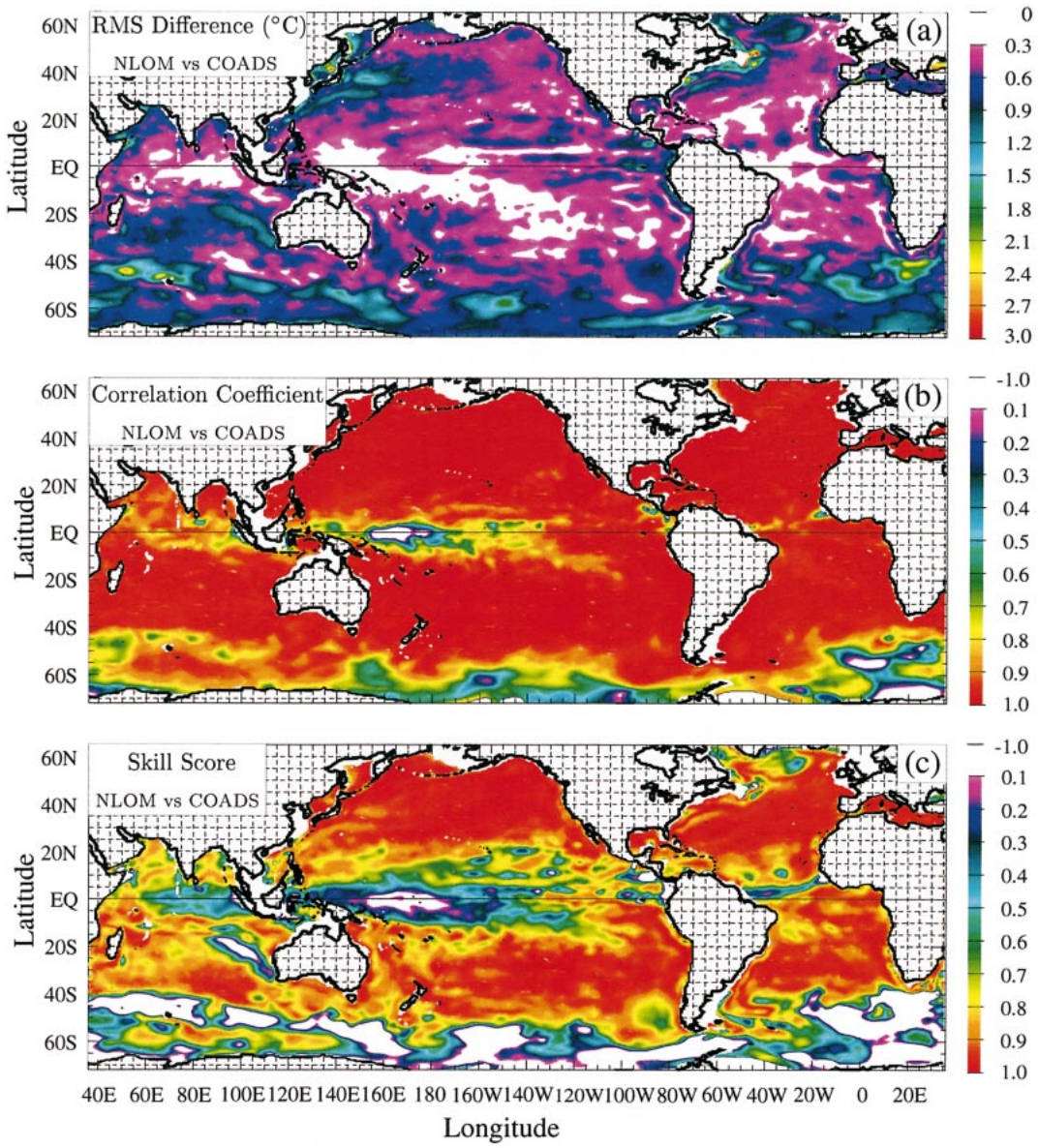

FIG. 3. Comparison of 12-month mean SST between COADS and NLOM at each model grid point over the global ocean. (a) The rms difference, (b) *R*, and (c) SS. Negative SS values indicate unskillfull results. In these comparisons COADS is treated as ''perfect''; thus, NLOM can never be more accurate than COADS. Global mean values for rms difference, *R*, and SS are 0.59°C, 0.91, and 0.68, respectively.

than ±0.5°C are negligible. Having small bias values is also evident from the zonally averaged ME map (Fig. 2).

We also examine the seasonal cycle of model SST with respect to climatology using rms difference (Fig. 3a), *R* (Fig. 3b), and SS (Fig. 3c) over the global ocean. The global rms difference between NLOM SST and COADS SST is 0.59°C. The shape of the seasonal cycle of the model SST is predicted very well as seen from the *R* values, which are close to 1 over most of the global ocean. The global *R* value is 0.91. Although the annual mean model SST is very close to the climatology in the Antarctic Ocean and equatorial warm pool, the seasonal cycle is not well predicted as evident from *R* values less than 0.5. Especially at the warm pool, none of these *R* values are significant at the 95% confidence interval. However, the rms difference is small due to the low amplitude (standard deviation) of the SST seasonal cycle in this region. The model also lacks any salinity input.

As explained in Seager et al. (1988), away from the equatorial region the SST is primarily determined by a one-dimensional balance of heat storage in the mixed layer and surface heat flux, resulting in a simple annual

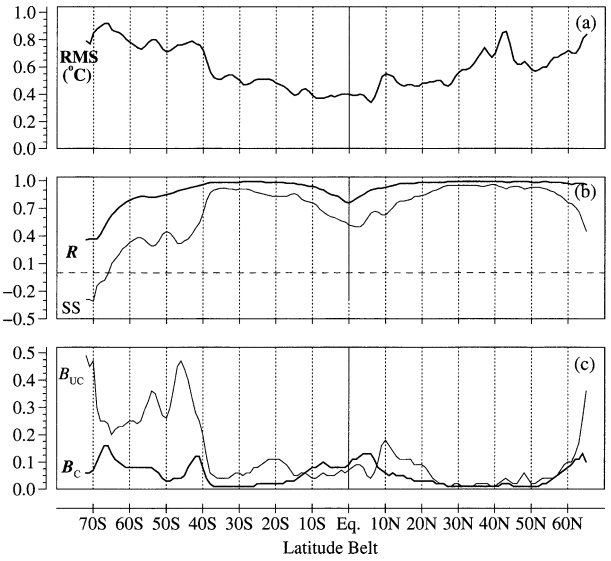

FIG. 4. The zonal averages of the fields shown in Fig. 3. Also shown are the zonal averages of the conditional and unconditional biases. (a) The rms difference in °C, (b) R (shown as bold line) and SS, and (c) B_C (shown as a bold line and B_{UC}. The zonal averaging is performed at each 1° latitude belt from 72°S to 65°N over the global ocean.

cycle of temperature. Strong cooling by latent heat flux loss occurs in the central parts of the ocean during summer and fall when the northeast trades are very strong and the South Pacific convergence zone is very weak. In the Northern Hemisphere, this results in the development of a tongue of cold water following the core of the trades, while in the Southern Hemisphere the cooling is responsible for destroying the southeastward extension of the western Pacific warm pool. In the Antarctic Ocean, one reason for having relatively low R values between the NLOM SST and COADS SST is that the NLOM is not able to correctly predict the MLD in this region due to the presence of ice and NLOM does not have ice. Errors in the sparsely observed forcing fields (e.g., Kent et al. 1993, da Silva et al. 1994) used by the model are another source of error in the Antarctic seasonal cycle.

The dimensionless SS (see Fig. 3c) is also a very informative measure of model performance in predicting SST because it takes bias into account, something that is not done by R. Note that part of the reduction in the SS values in comparison to correlation stems from the squaring of correlation in SS calculation. Biases are taken into account in the rms differences, but the latter can be small where SS and R are poor as in the central equatorial ocean because the amplitude of the seasonal cycle is small. Overall, NLOM's in predicting the SST is evident from the SS map with values being positive over most of the global ocean. The global average of SS is very high with a value of 0.67, indicating overall model success.

Another SST evaluation method is to examine zonally averaged error distribution for the SST seasonal cycle over the global ocean. For this purpose, zonal averages of the statistical measures discussed above (i.e., rms difference, R, SS, B_C and B_{UC}) are calculated at each 1° latitude belt from 65°N to 72°S and shown in Fig. 4. The rms difference is never greater than 1°C. NLOM usually yields $R > 0.7$, indicating statistically significant R values. The SS values are positive at all latitude belts, clearly indicating that NLOM is able to predict the seasonal cycle of SST reasonably well. The B_{UC} values (i.e., bias due to differences in the means of NLOM and COADS SSTs) are as large as 0.4 over a latitude belt, resulting in some of the lowest SS values occurring in the global ocean between 40° and 50°S. The B_C values represent a measure of the relative amplitude of the variability between the model and COADS. Obviously, they are very small in comparison to B_{UC} values. In these cases, the global B_{UC} and B_C are 0.12 and 0.05, respectively.

Finally, errors inherent in the COADS SST also affect the model comparisons presented in this paper. For example, in creating the COADS climatology there were ample SST data in the Northern Hemisphere, while the same was not true for the Southern Hemisphere (da Silva et al. 1994). Because the climatology is less accurate in the Southern Hemisphere we repeated the statistical analysis for the region that is north of 20°S and found that the rms difference for the SST seasonal cycle dropped to 0.53°C from the 0.59°C over the global domain. In addition, the global R value increased from 0.91 to 0.95 and the global SS value went from 0.67 to 0.80.

b. Mixed layer depth

In this section monthly mean MLD values obtained from the NLOM are compared to those obtained from the NRL mixed layer depth climatology (hereinafter referred to NMLD). This climatology (Kara et al. 2003) was constructed using temperature and salinity profiles from the *World Ocean Atlas* (Levitus et al. 1994; Levitus and Boyer 1994). In the NMLD, the MLD is described as the depth at the base of an isopycnal layer, where the density has changed by an amount of $\Delta\sigma_t = \sigma_t(T + \Delta T, S, P) - \sigma_t(T, S, P)$, where $P = 0$, from the density at a reference depth of 10 m that is consistent with the minimum NLOM depth. Based on Kara et al. (2000a) ΔT is the chosen optimal temperature difference with a value of 0.8°C.

Similar to the SST, we first examine the ability of model to predict the annual mean MLD in comparison to the NMLD climatology (Fig. 5a). NLOM is able to simulate MLD quite well over most of the global ocean (Fig. 5b). The global ME and rms differences between the NLOM MLD and NMLD are 9 and 34 m, respectively. At high latitudes, including some parts of the Antarctic Ocean and the North Atlantic Ocean, NLOM performs poorly in predicting mean MLD. Lack of sa-

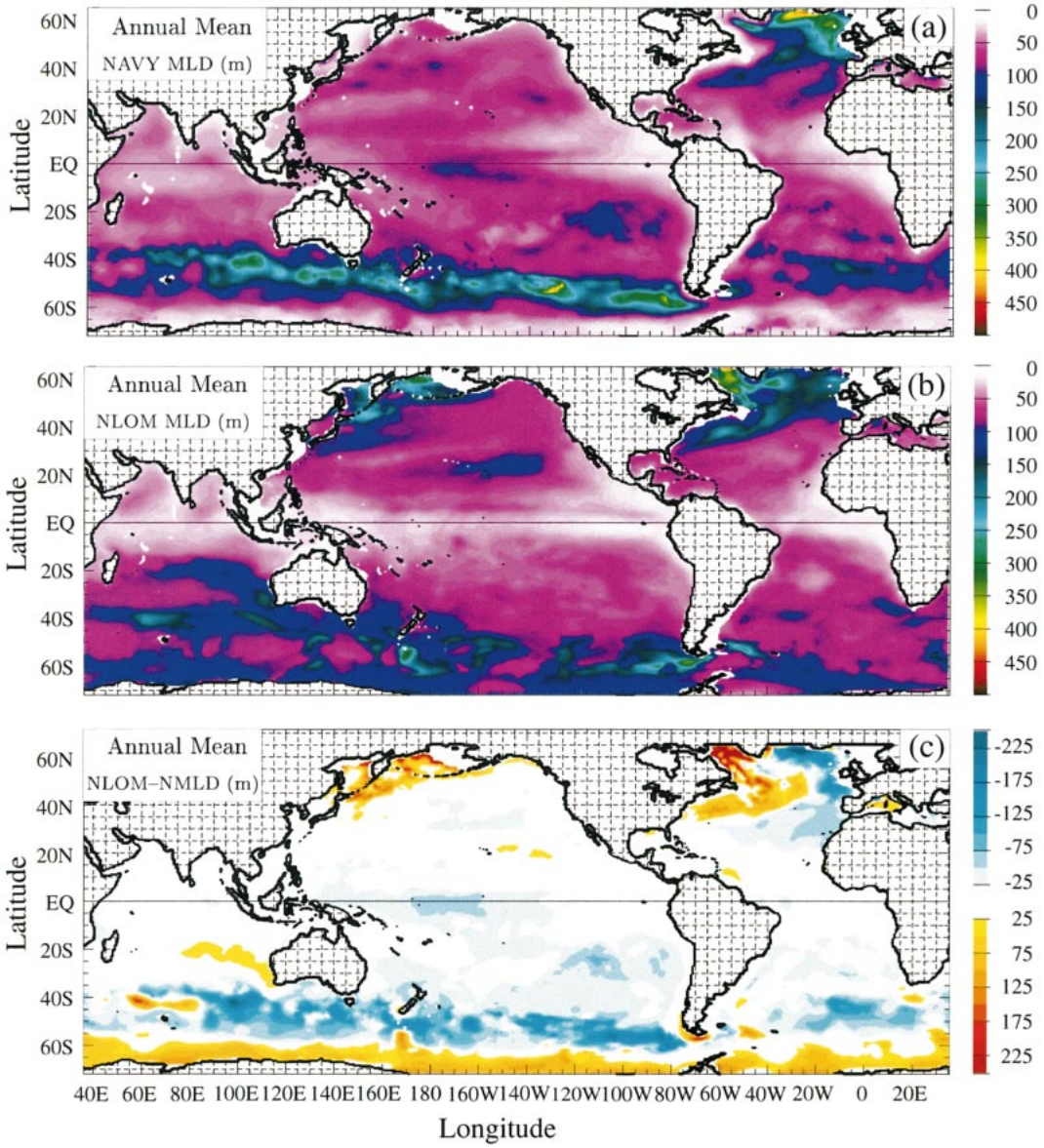

FIG. 5. Comparison of annual mean surface ocean MLD at each model grid point over the global ocean. (a) Annual mean climatological MLD from NMLD, (b) annual mean simulated MLD from NLOM, and (c) annual mean difference (ME) between the NLOM MLD and NMLD. Global average of annual MLD mean difference is 9 m, and the rms difference is 34 m.

linity forcing in the model and nonexistence of a special treatment for the sea ice fluxes are likely factors. Note here that the weaker stratification in the Southern Ocean enhances the relative importance of brine convection in the melting of Antarctic ice (e.g., Parkinson 1991) and the climatological MLD is very shallow in the Antarctic Ocean due to salinity stratification (e.g., Webster 1994). Deep mixed layers in the North Pacific Ocean and North Atlantic Ocean between 30° and 50°N are simulated reasonably well except for a few regions around the Gulf Stream and Kuroshio. Resolution of ½° is not adequate for realistic simulation of these current systems (Hurlburt et al. 1996; Hurlburt and Metzger 1998; Hurlburt and Hogan 2000). In general, the ME map between NLOM MLD and NMLD (Fig. 5c) shows that the model is able to produce an annual mean MLD with an error of 25 m or less over most of the global ocean, while the error is relatively large at high latitudes (Fig. 6).

The same statistical measures used for evaluating NLOM SST (see section 3a) are used for the seasonal cycle of the model MLD except that we first transform all NLOM MLD and NMLD values using a natural logarithmic (ln) function. The reason for this transformation is that winter MLDs are usually much deeper than

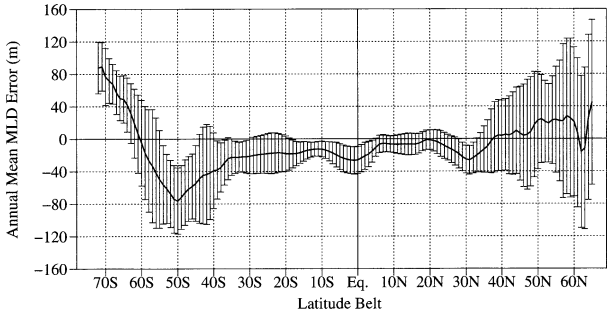

FIG. 6. The zonally averaged annual mean differences between NLOM MLD and NMLD values (see Fig. 5c). The annual mean is calculated using 12-monthly averages from Jan to Dec at each model grid point, and the zonal averaging is performed at each 1° latitude belt from 72°S to 65°N over the global ocean. Also included are the ± std devs of the zonally averaged annual mean differences for each latitude belt.

summer MLDs in both hemispheres. Thus, there is a skewed distribution for MLD values (i.e., much larger deviations above the mean than below the mean). The logarithmic transformation is applied to each of the 12 monthly NMLD and NLOM MLD values at every model grid over the global ocean. The purpose is to make the distribution of deviations more symmetric about the mean so that we can use the same measures that were used earlier for SST evaluation. Here it should be noted that power transforms are commonly used when all values are positive or negative (Bendat and Piersol 1986). Since the distribution is positively skewed (long tail for larger values) in our case, we can write $\mathrm{MLD}_{\mathrm{new}} = [\mathrm{MLD}_{\mathrm{old}}^{l}]$, where l is a real number less than zero. This is in the same family of transformations as $\mathrm{MLD}_{\mathrm{new}} = \ln[\mathrm{MLD}_{\mathrm{old}}]$, the transformation applied here to both the NMLD and NLOM MLD values.

The NLOM performance in predicting the seasonal cycle of MLD is shown in Fig. 7. Large rms differences are seen at high northern and southern latitudes (Fig. 7a). Some of these differences are due to sparse temperature and salinity data used in constructing the NMLD climatology. The impact of data density is clearly evident in Figs. 7b and 7c where the NLOM to NMLD comparisons tend to be much better in regions of relatively abundant data. For example, NLOM simulates the seasonal cycle of MLD in the North Pacific and North Atlantic Oceans quite well (Fig. 7b). The strong seasonal deepening and shallowing of the MLD from mid- to high latitudes are reproduced and this is also evident from the R and SS values between 20° and 50°N (Fig. 7). The rms difference and B_{UC} values between NLOM MLD and NMLD are relatively large in the equatorial ocean, resulting in SS values as low as 0.1 (Fig. 8). Although MLD rms differences are large north of about 40°N, which is due to large variability of the MLD in the North Atlantic, relatively large R and SS values show model success in this region.

As indicated in section 2, the minimum MLD was set to 10 m in the model. A few additional experiments were performed to test the sensitivity of the model results to the minimum value of MLD chosen (not shown). These used minimum MLD values ranging from 5 to 50 m. A thicker mixed layer (ML) should heat up more slowly, but this is balanced out by the feedback between SST and heat flux. We concluded that the model does not exhibit significant sensitivity to changes in the minimum surface MLD because the SST produced in all cases was almost equal to our standard model run. Overall, we noted only negligible cooling of SST < 0.05°C in the equatorial ocean with minimum MLD > 10 m. A possible reason is that the equatorial upwelling was increased because the temperature at the base of the mixed layer was reduced slightly. In addition, the surface heat flux is downward over most of the equator so a deeper surface layer results in a cooler SST.

4. Comparisons against buoy climatologies

Although the model results were verified against global climatologies of COADS for SST and NMLD for MLD, it is useful to compare the monthly means obtained from the model and the climatologies with those obtained at locations where there are long time series of data, for example, moored buoys, repeated transects, or ocean weather ships.

a. Buoy SST comparisons

Monthly mean SSTs from NLOM and the COADS climatology are compared to climatologies of monthly mean SST derived from time series at the locations shown in Fig. 9. These climatologies include 11 hydrographic stations in the North Pacific Ocean [hereinafter referred to as ocean weather station (OWS) climatologies] and 18 buoy locations along the U.S. coast, Hawaii, Alaska, and the Gulf of Mexico [hereinafter referred to as National Oceanic Data Center (NODC) climatologies]. A description of the OWS climatology can be found in Tabata and Weichselbaumer (1992). The reader is also referred to Table 2 for the time interval over which the climatology was constructed for each location. It should be noted that we only used buoys away from the coast where the ocean depth is greater than 200 m, which is the model boundary isobath.

Annual cycles of SST at selected locations from the OWS, NODC, and COADS climatologies are shown in Fig. 10, along with the annual cycle of SST simulated by the NLOM. For model–data comparisons, SST time series from OWS and NODC buoys are taken as reference values. The modeled SSTs are in good agreement with climatology throughout the year. Any systematic biases are small with modeled temperatures sometimes warmer and sometimes colder than climatological SST. A summary of statistics (Table 3) between the simulated climatological SST from the model and climatological NODC SST values for the buoy locations clearly indicates NLOM SST simulation skill as evident from ME

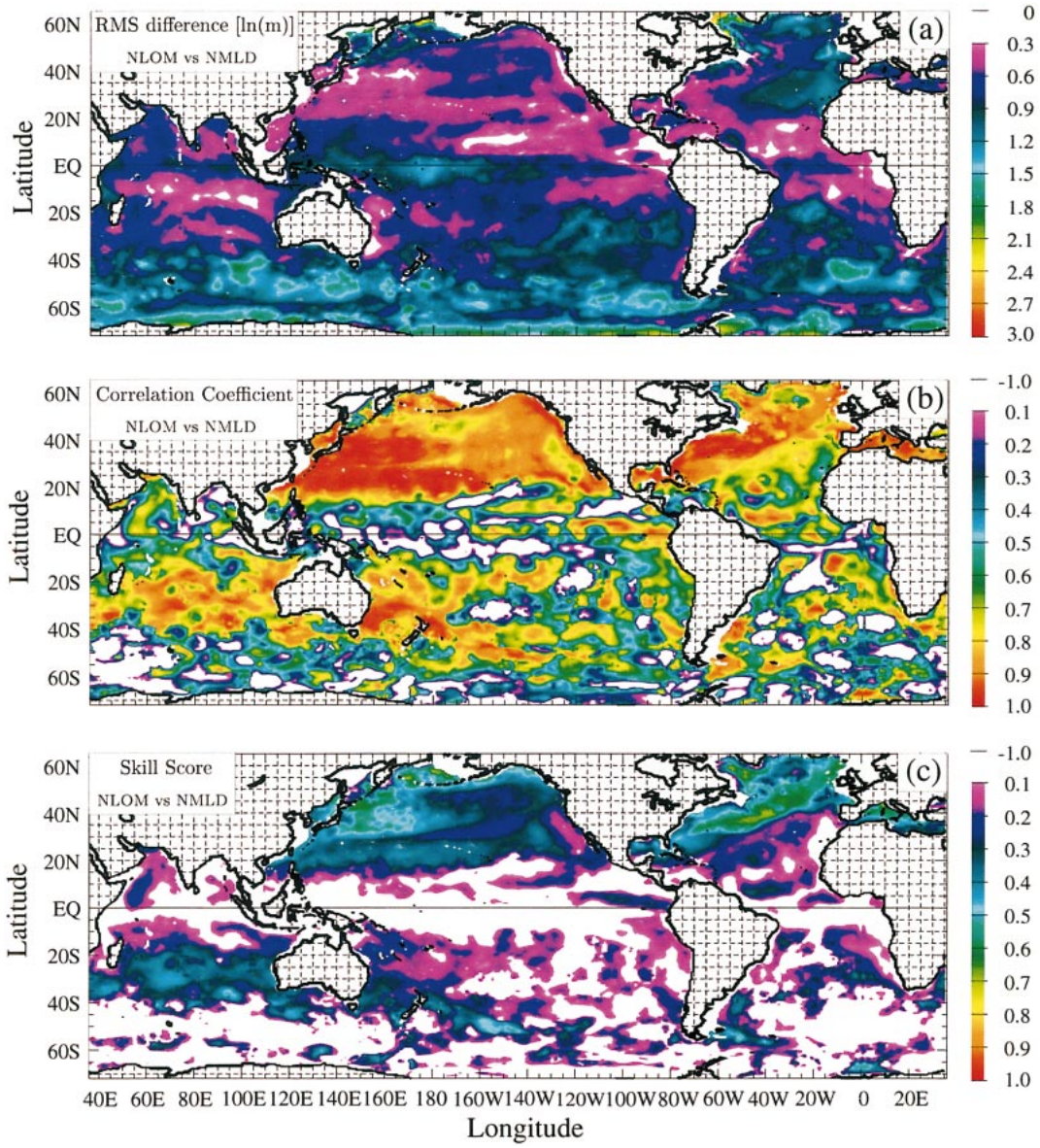

FIG. 7. Comparison of 12-month mean surface ocean MLDs between the NMLD climatology and NLOM at each model grid point over the global ocean. All climatological and model values are transformed to new values using ln tranformation as explained in the text. (a) The logarithmic rms difference, (b) *R*, and (c) SS. In these comparisons NMLD is treated as perfect. Thus NLOM can never be more accurate than NMLD.

values that are mostly smaller than ± 0.5°C and the large SS values that are close to 1 at most locations. The NLOM is able to simulate climatological SST very well, especially for buoys located north of 35°N (Table 4).

The seasonal cycle of NLOM SST is also compared to results from other mixed layer models reported in the literature. Most of those models are one-dimensional and their results were based on interannual simulations (Price et al. 1986). Such comparions are still useful because they report monthly mean differences over time periods as long as 20 yr. For example, Gaspar (1988) showed bulk mixed layer models systematically overestimate (underestimate) SST in summer (fall) because of heat flux forcing. This is not evident in the results presented here (see Fig. 10), at least for the buoys analyzed in this study. In Fig. 10 the difference between the NLOM SST and the OWS SST remains smaller than 0.5°C at most locations, and the largest ME value does not exceed 0.8°C. Using climatological advection of heat and salt for balancing heat and salt budgets in a model based on the K-profile parameterization (KPP), Webster et al. (1994) also obtained small SST errors in their simulations. Using a bulk-type mixed layer model, Price et al. (1986) showed a systematic bias in the sim-

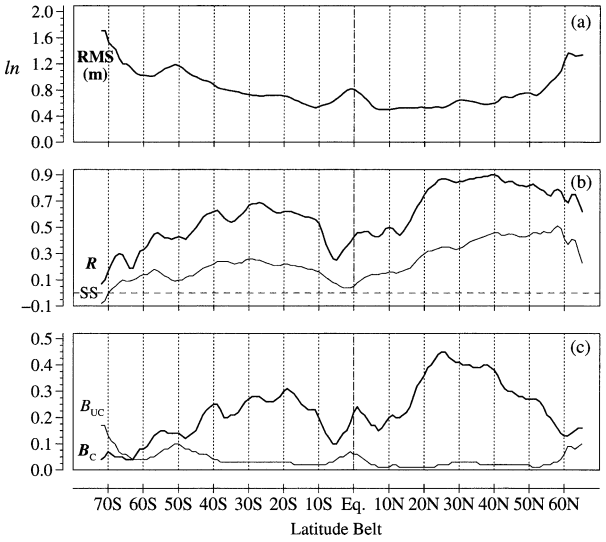

FIG. 8. The zonal averages of the fields shown in Fig. 7. Also shown are the zonal averages of the conditional and unconditional bias. (a) The rms difference in m, (b) R (shown as a bold line) and SS, and (c) B_C (shown as a bold line) and B_{UC}. The zonal averaging is performed at each 1° latitude belt from 72°S to 65°N over the global ocean.

ulations, and a serious underestimation of the monthly mean SST is evident even though they included climatological advection in the model simulations. The NLOM mixed layer model does not use salinity as an input in its simulations, but it is still able to predict climatological SST well.

For verification purposes, most of the model studies mentioned above used OWS Papa located at (50°N, 145°W). This has been an attractive location for one-dimensional mixed layer model studies because horizontal advective effects are relatively small in the northeast Pacific Ocean (Gill and Niiler 1973). We obtain very small rms difference and ME values of 0.33° and 0.18°C, respectively, at OWS Papa. Note that at the same location the rms difference and ME between the OWS SST and COADS SST (0.25° and 0.22°C, respectively) are close to the values calculated between NLOM and OWS SSTs. In addition to OWS Papa, we extend our statistical analysis to include other hydrographic locations in the northeast Pacific Ocean (Table 5). Model success is evident at all of these locations.

Overall, climatological error statistics are calculated using all 29 OWS and NODC locations. The results show that the median RMS and ME between the NLOM SST and buoy SST are 0.49° and −0.12°C, respectively. The median SS value is also very high with a value of 0.96. The same error statistics is also calculated comparing the NLOM and COADS SST annual cycles. The median RMS, ME, and SS between the NLOM and COADS SSTs are 0.29°C, −0.08°C, and 0.99, respectively. For reference, the median RMS, ME, and SS between COADS versus the buoy and OWS SSTs are 0.29°C, −0.07°C, and 0.99, respectively. This indicates

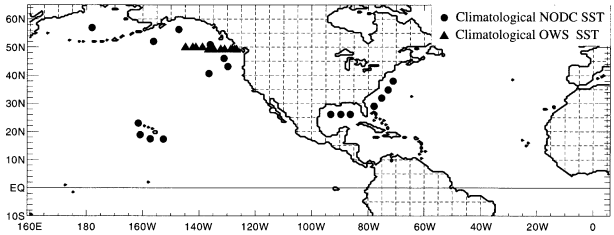

FIG. 9. OWS and NODC buoy locations. The reader is referred to Table 2 for further information about each individual buoy.

that some of the errors presented as model errors are due partly to errors in the COADS climatology.

One other useful measure of NLOM success is the ME in terms of surface heat fluxes. The total heat flux at the ocean surface, Q_n, varies with SST approximately according to $\partial Q_n/\partial \mathrm{SST} = (5 + 4\mathbf{v}_a)\ \mathrm{W\ m^{-2}\ K^{-1}}$, where the first term on the right-hand side comes from the longwave radiation, and the second term is due to the

TABLE 2. Climatological data information obtained from NODC buoys and OWS hydrographic locations. The OWS climatologies were constructed using monthly mean SSTs measured in different years from 1959 to 1990 (Tabata and Weichselbaumer 1992), while the NODC climatologies were constructed using daily SSTs available for the time intervals given here. The location at 50°N, 145°W is Ocean Weather Station Papa.

Lat, lon	NODC buoy locations	Depth of sea (m)	Climatology constructed
17°N, 153°W	Hawaii coast	5304	1984–94
17°N, 158°W	Hawaii coast	5002	1984–93
19°N, 161°W	Hawaii coast	4943	1984–93
23°N, 162°W	Hawaii coast	3257	1981–93
26°N, 86°W	Gulf of Mexico	3164	1976–93
26°N, 90°W	Gulf of Mexico	3246	1975–93
26°N, 94°W	Gulf of Mexico	3200	1973–93
29°N, 79°W	South Florida	823	1988–93
32°N, 75°W	Southeast United States	3786	1975–93
35°N, 73°W	Southeast United States	4389	1976–93
38°N, 71°W	Southeast United States	3164	1977–93
41°N, 137°W	Northwest United States	4023	1978–93
43°N, 130°W	Northwest United States	3420	1975–93
46°N, 131°W	Northwest United States	2853	1976–93
51°N, 136°W	Alaska coast	3529	1976–88
52°N, 156°W	Alaska coast	4572	1976–93
56°N, 148°W	Alaska coast	4206	1972–93
57°N, 178°W	Alaska coast	3611	1985–93

Lat, lon	OWS hydrographic stations	Depth of sea (m)	Climatology constructed
49°N, 127°W	Pacific Ocean	1300	1959–90
49°N, 128°W	Pacific Ocean	2500	1959–90
49°N, 129°W	Pacific Ocean	2440	1959–90
49°N, 131°W	Pacific Ocean	3300	1959–90
49°N, 133°W	Pacific Ocean	3275	1959–90
49°N, 135°W	Pacific Ocean	3550	1959–90
49°N, 137°W	Pacific Ocean	3775	1959–90
50°N, 139°W	Pacific Ocean	3890	1959–90
50°N, 141°W	Pacific Ocean	3880	1959–90
50°N, 143°W	Pacific Ocean	3910	1959–90
50°N, 145°W	Pacific Ocean	4200	1959–90

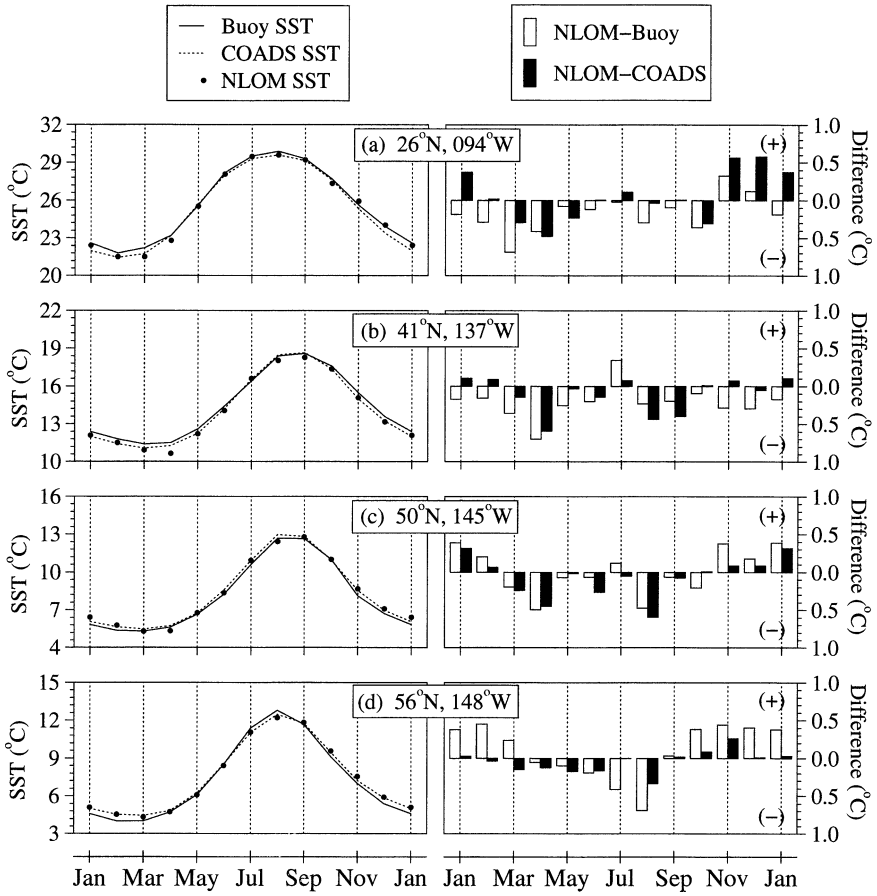

FIG. 10. Comparisons of NLOM-simulated SST to buoy SST at selected locations from the NODC and OWS climatologies. Also included are NLOM deviations from the climatologies. See Tables 3–5 for statistical results at all locations.

combined effects of the latent and sensible heat fluxes. Considering that the mean wind speed magnitude at buoy locations is about 10 m s^{-1}, an SST error of even 0.5°C can lead to flux errors of more than 20 W m^{-2}. This implies that a necessary, but insufficient, condition might be that the difference between the NLOM and buoy SST magnitudes (i.e., ME values) be less than 0.5°C for each month. Since annual ME values between the NLOM and buoy SSTs are usually less than ± 0.5 (see Tables 3, 4, and 5), this again indicates that NLOM successfully simulates climatological SST at the buoy locations.

b. Buoy MLD comparisons

Subsurface temperature and salinity are not available from the NODC climatologies; thus, we compare only the seasonal cycle of the simulated NLOM MLD against that of the climatological MLD from OWS hydrographic locations. The climatological MLD at each of the 11 OWS hydrographic stations (see Table 2) is calculated using monthly mean subsurface temperature and salinity data from 1959 to 1990. Monthly means of OWS temperature and salinity are averaged at each standard level over a 31-yr period. The standard levels used in the OWS dataset are all at 10-m increments from the surface to a depth of 1000 m. The reader is also referred to Kara et al. (2000a, c) who explain the MLD calculations at these OWS locations in detail.

Table 6 shows MLD annual cycle comparisons at OWS hydrographic stations. Also included in the table are comparions with the NMLD climatology that we previously used for verifying NLOM MLD over the global ocean. Note that normalized RMS is calculated as $\text{NRMS}^2 = 1/n \sum_{i=1}^{n} [(Y_i - X_i)/X_i]^2$, where $X_i (i = 1, 2, \ldots, n)$ is the set of n MLD values from the OWS and $Y_i (i = 1, 2, \ldots, n)$ is the set of MLD estimates from the NLOM. The reason for calculating an NRMS is that MLD can vary greatly from one season to another one (e.g., winter to summer); thus, we would like to normalize actual MLD values to examine percentage errors by NLOM. The median RMS and ME values between the NLOM MLD and OWS MLD are 20 and 12 m, respectively. Similarly, the median R and NRMS values are 0.86 and 0.39, respectively. In the case of NMLD versus NLOM MLD the median RMS, ME, R, and NRMS values are 19 m, 13

TABLE 3. Comparisons of the annual cycle of model-simulated SST with the NODC climatology (buoy vs NLOM), model-simulated SST with the COADS climatology (COADS vs NLOM); and COADS climatology with the NODC climatology (buoy vs COADS). All statistical measures are calculated using 12-monthly mean values. The std devs of the SST annual cycle are also given. Note that in the table X and Y denote independent and dependent variables considered in the calculations. For example, for (buoy vs NLOM), X denotes buoy, and Y denotes NLOM. All R values (not shown) are greater than 0.97 and statistically significant in comparison to a 0.7 correlation value at a 95% confidence interval. See section 3 for description of statistical measures.

Location	Comparisons of SST annual cycle	Rms (°C)	ME (°C)	σ_X (°C)	σ_Y (°C)	SS
17°N, 153°W	Buoy vs NLOM	0.67	−0.63	0.93	0.78	0.45
	COADS vs NLOM	0.47	−0.41	0.75	0.78	0.60
	Buoy vs COADS	0.47	−0.42	0.93	0.75	0.74
17°N, 158°W	Buoy vs NLOM	0.69	−0.56	0.90	0.70	0.41
	COADS vs NLOM	0.53	−0.47	0.76	0.70	0.51
	Buoy vs COADS	0.22	−0.09	0.90	0.76	0.94
19°N, 161°W	Buoy vs NLOM	0.54	−0.50	1.07	0.91	0.72
	COADS vs NLOM	0.18	−0.16	0.88	0.91	0.95
	Buoy vs COADS	0.41	−0.35	1.07	0.88	0.85
23°N, 162°W	Buoy vs NLOM	0.53	−0.47	1.43	1.22	0.85
	COADS vs NLOM	0.42	−0.36	1.36	1.22	0.91
	Buoy vs COADS	0.20	−0.11	1.43	1.36	0.98
26°N, 86°W	Buoy vs NLOM	1.13	−1.06	1.82	2.89	0.27
	COADS vs NLOM	0.69	−0.46	2.48	2.89	0.92
	Buoy vs COADS	0.92	−0.60	1.82	2.48	0.74
26°N, 90°W	Buoy vs NLOM	0.65	−0.16	2.65	3.01	0.94
	COADS vs NLOM	0.60	−0.37	2.66	3.01	0.95
	Buoy vs COADS	0.38	0.21	2.65	2.66	0.98
26°N, 94°W	Buoy vs NLOM	0.31	−0.17	2.91	2.99	0.99
	COADS vs NLOM	0.33	0.08	3.00	2.99	0.99
	Buoy vs COADS	0.32	−0.25	2.91	3.00	0.99
29°N, 79°W	Buoy vs NLOM	0.99	−0.62	2.14	2.68	0.79
	COADS vs NLOM	0.72	−0.54	2.30	2.68	0.90
	Buoy vs COADS	0.34	−0.08	2.14	2.30	0.97
32°N, 75°W	Buoy vs NLOM	0.59	0.04	2.45	2.78	0.94
	COADS vs NLOM	0.44	0.19	2.70	2.78	0.97
	Buoy vs COADS	0.35	−0.16	2.45	2.70	0.98

TABLE 4. Same as in Table 3 but for NODC buoys located north of 35°N.

Location	Comparisons of SST annual cycle	Rms (°C)	ME (°C)	σ_X (°C)	σ_Y (°C)	SS
35°N, 73°W	Buoy vs NLOM	0.70	0.13	2.53	2.96	0.92
	COADS vs NLOM	0.78	0.61	3.27	2.96	0.94
	Buoy vs COADS	0.92	−0.48	2.53	3.27	0.87
38°N, 71°W	Buoy vs NLOM	1.34	−1.05	4.27	3.76	0.90
	COADS vs NLOM	0.88	0.03	4.31	3.76	0.96
	Buoy vs COADS	1.12	−1.08	4.27	4.31	0.93
41°N, 137°W	Buoy vs NLOM	0.41	−0.35	2.60	2.71	0.97
	COADS vs NLOM	0.25	−0.12	2.74	2.71	0.99
	Buoy vs COADS	0.30	−0.23	2.60	2.74	0.99
43°N, 130°W	Buoy vs NLOM	0.77	−0.70	2.59	2.51	0.91
	COADS vs NLOM	0.33	−0.23	2.45	2.51	0.98
	Buoy vs COADS	0.52	−0.48	2.59	2.45	0.96
46°N, 131°W	Buoy vs NLOM	0.58	−0.41	2.68	2.88	0.95
	COADS vs NLOM	0.26	−0.08	2.74	2.88	0.99
	Buoy vs COADS	0.43	−0.32	2.68	2.74	0.97
51°N, 136°W	Buoy vs NLOM	0.27	0.07	2.67	2.70	0.99
	COADS vs NLOM	0.25	−0.01	2.66	2.70	0.99
	Buoy vs COADS	0.26	0.08	2.67	2.66	0.99
52°N, 156°W	Buoy vs NLOM	0.40	0.34	2.71	2.56	0.98
	COADS vs NLOM	0.21	−0.05	2.72	2.56	0.99
	Buoy vs COADS	0.40	0.38	2.71	2.72	0.98
56°N, 148°W	Buoy vs NLOM	0.40	0.17	3.05	2.82	0.98
	COADS vs NLOM	0.15	0.00	2.83	2.82	1.00
	Buoy vs COADS	0.33	0.17	3.05	2.83	0.99
57°N, 178°W	Buoy vs NLOM	0.20	−0.10	2.60	2.56	0.99
	COADS vs NLOM	0.23	0.11	2.62	2.56	0.98
	Buoy vs COADS	0.25	−0.21	2.60	2.62	0.99

TABLE 5. Same as in Table 3 but for OWS hydrographic stations located in the northeast Pacific Ocean.

Location	Comparisons of SST annual cycle	Rms (°C)	ME (°C)	σ_X (°C)	σ_Y (°C)	SS
49°N, 127°W	OWS vs NLOM	0.53	−0.32	2.19	2.52	0.94
	COADS vs NLOM	0.32	−0.13	2.36	2.52	0.98
	OWS vs COADS	0.39	−0.39	2.19	2.36	0.97
49°N, 128°W	OWS vs NLOM	0.45	−0.10	2.54	2.82	0.97
	COADS vs NLOM	0.49	0.23	2.43	2.82	0.96
	OWS vs COADS	0.45	−0.33	2.54	2.43	0.97
49°N, 129°W	OWS vs NLOM	0.44	−0.11	2.73	2.83	0.97
	COADS vs NLOM	0.40	0.11	2.48	2.83	0.97
	OWS vs COADS	0.46	−0.22	2.73	2.48	0.97
49°N, 131°W	OWS vs NLOM	0.55	−0.29	2.86	2.78	0.96
	COADS vs NLOM	0.30	0.01	2.58	2.78	0.99
	OWS vs COADS	0.58	−0.29	2.86	2.58	0.96
49°N, 133°W	OWS vs NLOM	0.41	0.06	2.85	2.80	0.98
	COADS vs NLOM	0.30	0.07	2.66	2.80	0.99
	OWS vs COADS	0.39	−0.01	2.85	2.66	0.98
49°N, 135°W	OWS vs NLOM	0.52	0.04	2.87	2.78	0.97
	COADS vs NLOM	0.28	−0.05	2.70	2.78	0.99
	OWS vs COADS	0.50	0.09	2.87	2.70	0.97
49°N, 137°W	OWS vs NLOM	0.51	0.15	2.67	2.74	0.96
	COADS vs NLOM	0.28	−0.08	2.72	2.74	0.99
	OWS vs COADS	0.46	0.23	2.67	2.72	0.97
50°N, 139°W	OWS vs NLOM	0.41	0.25	2.66	2.73	0.98
	COADS vs NLOM	0.27	0.05	2.71	2.73	0.99
	OWS vs COADS	0.33	0.20	2.66	2.71	0.98
50°N, 141°W	OWS vs NLOM	0.41	0.12	2.64	2.73	0.98
	COADS vs NLOM	0.27	−0.02	2.71	2.73	0.99
	OWS vs COADS	0.39	0.13	2.64	2.71	0.98
50°N, 143°W	OWS vs NLOM	0.28	−0.07	2.68	2.70	0.99
	COADS vs NLOM	0.28	−0.15	2.70	2.70	0.99
	OWS vs COADS	0.28	0.09	2.68	2.70	0.99
50°N, 145°W	OWS vs NLOM	0.33	0.18	2.70	2.63	0.98
	COADS vs NLOM	0.25	−0.04	2.69	2.63	0.99
	OWS vs COADS	0.25	0.22	2.70	2.69	0.99

m, 0.87, and 0.38, respectively. Table 6 shows agreement between some pairs of OWS MLD versus NLOM MLD, while NMLD versus NLOM MLD is quite different. Comparing the OWS MLD versus NMLD, we find the median values for RMS, ME (NMLD–OWS MLD), *R*, and NRMS are 6 m, −2 m, 0.98, and 0.10, respectively.

More detailed comparisons of the seasonal cycle of MLD from NLOM, the OWS, and the NMLD are shown in Fig. 11 for selected stations. At these locations NLOM MLD is deeper than both OWS MLD and NMLD in winter and the NLOM annual cycle leads the observed annual cycle by approximately 15 days to 1 month, or ≈6%. The higher 10-m resolution of the OWS data enables the layer depths to be obtained more accurately than those calculated from the Levitus climatology. The OWS data also exhibit a shallower and sharper thermocline because there is no horizontal averaging of the temperature and salinity profiles as was done in creating the Levitus climatology.

5. Summary and conclusions

The purpose of this paper is to examine globally the performance of the Naval Research Laboratory (NRL) Layered Ocean Model (NLOM) in predicting climatological monthly mean sea surface temperature (SST) and ocean mixed layer depth (MLD), when forced by atmospheric climatologies with no relaxation toward observed SSTs. This includes detailed assessment of regional variations in performance. The model–data comparisons were made using both global ocean climatologies and climatologies calculated from long time series at particular locations. For a quantitative evaluation of the model performance, several statistical measures, such as mean error (ME), root-mean-square (rms) difference (RMS), correlation coefficient (*R*), and skill score (SS), were used. Using these measures, time series of monthly mean SST and MLD values from the NLOM were compared to those from the climatological fields at each model grid point over the global ocean. Spatial maps and zonal averages of each statistical measure were then generated to examine model performance.

Since the accuracy of the atmospheric forcing and the climatologies of SST and MLD can strongly affect quantitative measures of model simulation skill, high model simulation skill is also an assessment of these factors to a limited extent. Although many of these datasets were used in tuning the parameters of the mixed layer model, it would be difficult to obtain high model accuracy over the diverse regimes of the global ocean with

TABLE 6. Comparisons of the annual cycle of model-simulated MLD with the ones calculated from OWS climatological salinity and temperature (OWS vs NLOM), model-simulated MLD with NMLD (NMLD vs NLOM), and NMLD with OWS climatology (OWS vs NMLD). Kara et al. (2000a) explains details of density and MLD calculations from the observed temperature and salinity profiles.

Location	Comparisons of MLD annual cycle	Rms (°C)	ME (°C)	σ_X (°C)	σ_Y (°C)	R (X, Y)	NRMS (X, Y)
49°N, 127°W	OWS vs NLOM	21.4	10.5	17.1	23.3	0.86	0.43
	NMLD vs NLOM	23.3	14.9	14.8	23.3	0.73	0.45
	OWS vs NMLD	7.4	−4.3	17.1	14.8	0.92	0.20
49°N, 128°W	OWS vs NLOM	24.2	14.8	26.2	32.3	0.86	0.57
	NMLD vs NLOM	30.1	21.7	20.3	32.3	0.97	0.86
	OWS vs NMLD	12.5	−6.8	26.2	20.3	0.77	0.23
49°N, 129°W	OWS vs NLOM	19.8	11.1	16.7	32.0	0.89	0.41
	NMLD vs NLOM	28.3	19.9	12.3	32.0	0.97	0.70
	OWS vs NMLD	12.2	−8.8	16.7	12.3	0.87	0.25
49°N, 131°W	OWS vs NLOM	22.3	15.4	20.9	33.2	0.92	0.39
	NMLD vs NLOM	28.3	22.0	16.5	33.2	0.96	0.56
	OWS vs NMLD	8.9	−6.6	20.9	16.5	0.98	0.15
49°N, 133°W	OWS vs NLOM	22.2	12.8	24.4	32.9	0.84	0.39
	NMLD vs NLOM	21.5	15.1	22.4	32.9	0.92	0.38
	OWS vs NMLD	5.5	−2.3	24.4	22.4	0.98	0.10
49°N, 135°W	OWS vs NLOM	21.2	14.3	23.4	32.1	0.84	0.42
	NMLD vs NLOM	19.4	13.2	24.8	32.1	0.89	0.37
	OWS vs NMLD	4.8	1.2	23.4	24.8	0.98	0.08
49°N, 137°W	OWS vs NLOM	19.2	9.2	28.6	31.1	0.83	0.38
	NMLD vs NLOM	18.6	11.0	27.1	31.1	0.87	0.37
	OWS vs NMLD	4.8	−1.8	28.6	27.1	0.99	0.09
50°N, 139°W	OWS vs NLOM	20.2	11.5	27.8	30.2	0.83	0.43
	NMLD vs NLOM	17.8	10.1	26.1	30.2	0.87	0.37
	OWS vs NMLD	5.7	1.5	27.8	26.1	0.98	0.10
50°N, 141°W	OWS vs NLOM	19.5	13.5	25.4	25.4	0.85	0.35
	NMLD vs NLOM	16.8	12.4	27.2	25.4	0.86	0.33
	OWS vs NMLD	7.3	2.3	25.4	27.2	0.98	0.08
50°N, 143°W	OWS vs NLOM	18.9	11.9	28.2	29.8	0.86	0.40
	NMLD vs NLOM	19.3	12.7	28.2	29.8	0.87	0.41
	OWS vs NMLD	5.4	−0.8	28.2	28.2	0.99	0.11
50°N, 145°W	OWS vs NLOM	17.4	11.7	29.2	29.5	0.87	0.32
	NMLD vs NLOM	19.2	13.2	27.5	29.5	0.87	0.41
	OWS vs NMLD	3.7	−0.5	29.2	27.5	0.98	0.06

highly inaccurate data, and NLOM clearly shows more accurate results in the Northern Hemisphere than in the Southern Hemisphere. Climatologies of SST and MLD from data time series at fixed locations are used for independent verification. The thermal forcing and the ''observed'' MLD are particularly suspect. The ''poor'' quality of the thermal forcing is one reason why ocean modelers often relax their ocean model simulations to observed SST. Success in simulation of SST and MLD using atmospheric forcing with no relaxation to observed SST is a critical demonstration that the atmospheric forcing is adequate for this purpose.

One assessment of SST simulation skill is a comparison of the annual mean and seasonal cycle globally from 72°S to 65°N with the Comprehensive Ocean Atmosphere Data Set (COADS). Climatological SST error statistics using wind forcing from the Hellerman and Rosenstein (1983) wind stress climatology with 6-hourly variability added and monthly thermal forcing from COADS showed that NLOM gives a global rms difference of 0.37°C for the annual mean and 0.59°C for the seasonal cycle over the global ocean. The mean global R for the seasonal cycle of the SST is 0.91. The annual mean model SST is very close to the climatology in the Antarctic region and the equatorial warm pool, but the seasonal cycle is not well predicted because the amplitude of the seasonal cycle is so small, and the model lacks any salinity input in these regions where salinity plays a significant role in the mixed layer dynamics. The NLOM is also able to reproduce the MLD seasonal cycle moderately well, considering the fact that there are some limitations in the climatological MLD field used for verification purposes. Large SS values showed that deep winter mixed layers in the Atlantic Ocean and Southern Ocean are reproduced by the model, while relatively low SS values are evident at the equator. Overall, the rms differences between MLDs from NLOM and the ones from NRL MLD (NMLD) are 34 m for the annual mean and 63 m for the seasonal cycle. The mean global R value for the seasonal cycle of the MLD is 0.62.

Model–data comparisons were also performed using climatological monthly mean SST and MLD time series constructed from 11 ocean weather stations (OWSs) in the northeast Pacific and 18 National Oceanic Data Center (NODC) buoys located off of the U.S. coasts, Hawaii, Alaska, and in the Gulf of Mexico. Detailed statistical verification between NLOM and buoy time series

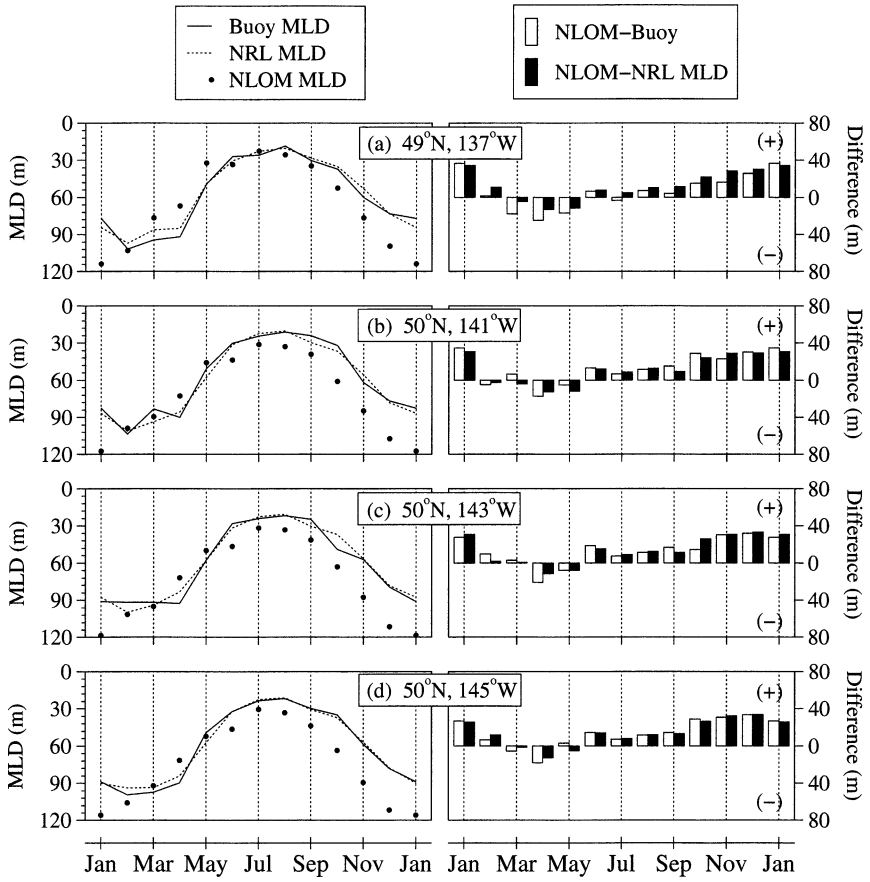

FIG. 11. Comparisons of NLOM-simulated MLD to buoy MLD at selected locations from the NMLD climatologies. Also included are deviations from the NLOM. See Table 6 for statistical results at all OWS locations.

was presented at each buoy and ocean weather station. Based on median SST error statistics from all 29 locations (i.e., twenty-nine 12-month-long time series), NLOM gives an rms difference of 0.49°C, an ME of −0.12°C, and an SS value of 0.96. The median *R* value is 0.99. Comparisons against buoy MLD values calculated from subsurface temperature and salinity profiles at the OWS stations located in the northeast Pacific Ocean also verify that NLOM is able to simulate the MLD seasonal cycle well, capturing the winter (summer) deepening (shallowing) with about 6% phase lead. The median RMS and ME values between the NLOM MLD and OWS MLD are 20 and 12 m, respectively. Similarly, the median *R* and NRMS values are 0.86 and 0.41, respectively.

Finally, it is noted that the global NLOM at 1/16° resolution became an operational ocean prediction product at the Naval Oceanographic Office (NAVOCEANO), Stennis Space Center, Mississippi, in September 2001. Real-time and archived results from the system can be seen online (http://www.ocean.nrlssc.navy.mil/global_nlom). This includes many zoom regions, nowcasts, and forecasts of upper-ocean quantities along with comparisons against independent data and forecast verification statistics.

Acknowledgments. We would like to thank to E. J. Metzger of the Naval Research Laboratory (NRL) at the Stennis Space Center for processing atmospheric forcing fields for the model runs. Constructive criticisms made by the reviewers are greatly appreciated. The ocean color data used in this paper were obtained from the Goddard Distributed Active Archive Center under the auspices of the National Aeronautics and Space Administration (NASA). Use of this data is in accord with the Sea-viewing Wide Field-of-view Sensor (SeaWiFS) Research Data Use Terms and Conditions Agreement. The numerical simulations were performed under the Department of Defense High Performance Computing Modernization Program on an SGI Origin 2000 and a Cray T3E at the Naval Oceanographic Office, Stennis Space Center, Mississippi, and on a Cray T3E at the Arctic Region Supercomputer Center, Fairbanks, Alaska. This work was funded by the Office of Naval Research (ONR) and is a contribution of the Basin-Scale Prediction System project under Program Element

602435N. This NRL/JA contribution has been approved for public release.

REFERENCES

Bendat, J. S., and A. G. Piersol, 1986: *Random Data: Analysis and Measurement Procedures.* Wiley and Sons, 566 pp.

Blanc, T. V., 1987: Accuracy of bulk method determined flux, stability, and sea surface roughness. *J. Geophys. Res.,* **92,** 3867–3876.

Cherniawsky, J. Y., and G. Holloway, 1991: An upper-ocean general circulation model for the North Pacific: Preliminary experiments. *Atmos.–Ocean,* **29,** 737–784.

da Silva, A. M., C. C. Young, and S. Levitus, 1994: *Algorithms and Procedures.* Vol. 1, *Atlas of Surface Marine Data 1994,* NOAA Atlas NESDIS 6, 83 pp.

Fairall, C. W., E. F. Bradley, D. P. Rogers, J. B. Edson, and G. S. Young, 1996: Bulk parameterization of air–sea fluxes for Tropical Ocean-Global Atmosphere Coupled-Ocean Atmosphere Response Experiment. *J. Geophys. Res.,* **101,** 3747–3764.

Garwood, R. W., 1977: An oceanic mixed layer model capable of simulating cyclic states. *J. Phys. Oceanogr.,* **7,** 455–468.

Gaspar, P., 1988: Modeling the seasonal cycle of the upper ocean. *J. Phys. Oceanogr.,* **18,** 161–180.

Gill, A. E., and P. P. Niiler, 1973: The theory of the seasonal variability in the ocean. *Deep-Sea Res.,* **20,** 141–177.

Hellerman, S., and M. Rosenstein, 1983: Normal monthly wind stress over the world ocean with error estimates. *J. Phys. Oceanogr.,* **13,** 1093–1104.

Hu, D., and Y. Chao, 1999: A global isopycnal OGCM: Validations using observed upper-ocean variabilities during 1992–1993. *Mon. Wea. Rev.,* **127,** 706–725.

Hurlburt, H. E., and E. J. Metzger, 1998: Bifurcation of the Kuroshio Extension at the Shatsky Rise. *J. Geophys. Res.,* **103,** 7549–7566.

——, and P. J. Hogan, 2000: Impact of 1/8° to 1/64° resolution on Gulf Stream model-data comparisons in basin-scale subtropical Atlantic Ocean models. *Dyn. Atmos. Oceans,* **32,** 283–329.

——, A. J. Wallcraft, W. J. Schmitz Jr., P. J. Hogan, and E. J. Metzger, 1996: Dynamics of the Kuroshio/Oyashio current system using eddy-resolving models of the North Pacific Ocean. *J. Geophys. Res.,* **101,** 941–976.

Jacobs, G. A., H. E. Hurlburt, J. C. Kindle, E. J. Metzger, J. L. Mitchell, W. J. Teague, and A. J. Wallcraft, 1994: Decade-scale trans-Pacific propagation and warming effects of an El Niño anomaly. *Nature,* **370,** 360–363.

Kantha, L. H., and C. A. Clayson, 1994: An improved mixed layer model for geophysical applications. *J. Geophys. Res.,* **99,** 25 235–25 266.

Kara, A. B., P. A. Rochford, and H. E. Hurlburt, 2000a: An optimal definition for ocean mixed layer depth. *J. Geophys. Res.,* **105,** 16 803–16 821.

——, ——, and ——, 2000b: Efficient and accurate bulk parameterizations of air–sea fluxes for use in general circulation models. *J. Atmos. Oceanic Technol.,* **17,** 1421–1438.

——, ——, and ——, 2000c: Mixed layer depth variability and barrier layer formation over the North Pacific Ocean. *J. Geophys. Res.,* **105,** 16 783–16 801.

——, ——, and ——, 2002a: Air–sea flux estimates and the 1997–1998 ENSO event. *Bound.-Layer Meteor.,* **103,** 439–458.

——, ——, and ——, 2002b: Naval Research Laboratory Mixed Layer Depth (NMLD) climatologies. NRL Rep. NRL/FR/7330-02-9995, 26 pp. [Available from Naval Research Laboratory, Code 7323, Stennis Space Center, MS 39529-5004.]

——, ——, and ——, 2003: Mixed layer depth variability over the global ocean. *J. Geophys. Res.,* **108,** 3079, doi:10.1029/2000JC000736.

Kent, E. C., P. K. Taylor, B. S. Truscott, and J. A. Hopkins, 1993: The accuracy of voluntary observing ships' meteorological observations—Results of the VSOP-NA. *J. Atmos. Oceanic Technol.,* **10,** 591–608.

Kraus, E. B., and J. S. Turner, 1967: A one-dimensional model of the seasonal thermocline: II. The general theory and its consequences. *Tellus,* **19,** 98–106.

Levitus, S., and T. P. Boyer, 1994: *Temperature.* Vol. 4, *World Ocean Atlas 1994,* NOAA Atlas NESDIS 4, 117 pp.

——, R. Burgett, and T. P. Boyer, 1994: *Salinity.* Vol. 3, *World Ocean Atlas 1994,* NOAA Atlas NESDIS 3, 99 pp.

Li, M., and C. Garrett, 1997: Mixed layer deepening due to Langmuir circulation. *J. Phys. Oceanogr.,* **27,** 121–132.

Martin, P., 1985: Simulation of the mixed layer at OWS November and Papa with several models. *J. Geophys. Res.,* **90,** 903–916.

Metzger, E. J., and H. E. Hurlburt, 1996: Coupled dynamics of the South China Sea, the Sulu Sea, and the Pacific Ocean. *J. Geophys. Res.,* **101,** 12 331–12 352.

Murphy, A. H., 1988: Skill scores based on the mean square error and their relationships to the correlation coeffient. *Mon. Wea. Rev.,* **116,** 2417–2424.

——, 1992: Climatology, persistence, and their linear combination as standards of reference in skill scores. *Wea. Forecasting,* **7,** 692–698.

——, and H. Daan, 1985: Forecast evaluation. *Probability, Statistics, and Decision Making in the Atmospheric Sciences,* A. H. Murphy and R. W. Katz, Eds., Westview Press, 379–437.

Murtugudde, R., M. Cane, and V. Prasad, 1995: A reduced-gravity, primitive equation, isopycnal ocean GCM: Formulation and simulations. *Mon. Wea. Rev.,* **123,** 2864–2887.

Neter, J., W. Wasserman, and G. A. Whitmore, 1988: *Applied Statistics.* Allyn and Bacon, 1006 pp.

Nicholls, N., 2001: The insignificance of significance testing. *Bull. Amer. Meteor. Soc.,* **82,** 981–986.

Niiler, P. P., and E. B. Kraus, 1977: One-dimensional models of the upper ocean. *Modeling and Prediction of the Upper Layers of the Ocean,* E. B. Kraus, Ed., Pergamon Press, 143–172.

Parkinson, C. L., 1991: Interannual variability of monthly Southern Ocean sea ice distribution. *J. Geophys. Res.,* **96,** 4791–4801.

Price, J. F., R. A. Weller, and R. Pinkel, 1986: Diurnal cycling: Observations and models of the upper ocean response to diurnal heating, cooling, and wind mixing. *J. Geophys. Res.,* **91,** 8411–8427.

Rochford, P. A., A. B. Kara, A. J. Wallcraft, and R. A. Arnone, 2001: Importance of solar subsurface heating in ocean general circulation models. *J. Geophys. Res.,* **106,** 30 923–30 938.

Schopf, P. S., and A. Loughe, 1995: A reduced-gravity isopycnal ocean model: Hindcasts of El Niño. *Mon. Wea. Rev.,* **123,** 2839–2863.

Seager, R., S. E. Zebiak, and M. A. Cane, 1988: A model of the tropical Pacific sea surface temperature climatology. *J. Geophys. Res.,* **93,** 1265–1280.

Stewart, T. R., 1990: A decomposition of the correlation coefficient and its use in analyzing forecasting skill. *Wea. Forecasting,* **5,** 661–666.

Tabata, S., and W. E. Weichselbaumer, 1992: An update of the statistics of oceanographic data based on hydrographic/CTD casts made at stations 1 through 6 along line P during January 1959 through September 1990. Canadian Data Rep. of Hydrography and Ocean Sciences No. 108, 317 pp.

Wallcraft, A. J., A. B. Kara, H. E. Hurlburt, and P. A. Rochford, 2003: The NRL Layered Global Ocean Model (NLOM) with an embedded mixed layer submodel: Formulation and tuning-simulations. *J. Atmos. Oceanic Technol.,* **20,** 1601–1615.

Webster, P. J., 1994: The role of hydrological processes in ocean–atmosphere interactions. *Rev. Geophys.,* **32,** 427–476.

Yuen, C. W., J. Y. Cherniawsky, C. A. Lin, and L. A. Mysak, 1992: An upper ocean general circulation model for climate studies: Global simulation with seasonal cycle. *Climate Dyn.,* **7,** 1–18.